

Published in final edited form as:

*J Hum Genet.* 2016 April ; 61(4): 295–300. doi:10.1038/jhg.2015.149.

## First Independent Replication of the Involvement of *LARS2* in Perrault Syndrome by Whole-Exome Sequencing of an Italian Family

Giulia Soldà<sup>1,2,\*</sup>, Sonia Caccia<sup>3</sup>, Michela Robusto<sup>1,2</sup>, Chiara Chiereghin<sup>1,2</sup>, Pierangela Castorina<sup>4</sup>, Umberto Ambrosetti<sup>4,5</sup>, Stefano Duga<sup>1,2</sup>, and Rosanna Asselta<sup>1,2</sup>

<sup>1</sup>Department of Biomedical Sciences, Humanitas University, Rozzano, Milan, Italy

<sup>2</sup>Humanitas Clinical and Research Center, Rozzano, Milan, Italy

<sup>3</sup>Department of Biomedical and Clinical Sciences "Luigi Sacco", Università degli Studi di Milano - LITA Vialba, Milan, Italy

<sup>4</sup>UO Audiologia, Fondazione IRCCS Cà Granda Ospedale Maggiore Policlinico, Milan, Italy

<sup>5</sup>Dipartimento di Scienze Cliniche e di Comunità, Università degli Studi di Milano, Milan, Italy

### Abstract

Perrault syndrome (MIM #233400) is a rare autosomal recessive disorder characterized by ovarian dysgenesis and primary ovarian insufficiency in females, and progressive hearing loss in both genders. Recently, mutations in five genes (*HSD17B4*, *HARS2*, *CLPP*, *LARS2*, and *C10ORF2*) were found to be responsible for Perrault syndrome, although they do not account for all cases of this genetically heterogeneous condition.

We used whole-exome sequencing to identify pathogenic variants responsible for Perrault syndrome in an Italian pedigree with two affected siblings. Both patients were compound heterozygous for two novel missense variants within the mitochondrial leucyl-tRNA synthetase (*LARS2*, NM\_015340.3:c.899C>T(p.Thr300Met) and c.1912G>A(p.Glu638Lys). Both variants co-segregated with the phenotype in the family. p.Thr300 and p.Glu638 are evolutionary conserved residues, and are located respectively within the editing domain and immediately before the catalytically important KMSKS motif. Homology modeling using as template the *E. coli* leucyl-tRNA synthetase provided further insights on the possible pathogenic effects of the identified variants.

This represents the first independent replication of the involvement of *LARS2* mutations in Perrault syndrome, contributing valuable information for the further understanding of this disease.

---

Users may view, print, copy, and download text and data-mine the content in such documents, for the purposes of academic research, subject always to the full Conditions of use:[http://www.nature.com/authors/editorial\\_policies/license.html#terms](http://www.nature.com/authors/editorial_policies/license.html#terms)

\***Corresponding author:** Giulia Soldà, PhD, Assistant Professor of Applied Biology, Department of Biomedical Sciences, Humanitas University and Humanitas Clinical and Research Center, 20089 Rozzano, Milan – Italy, phone: +39 02 82245216, [giulia.solda@hunimed.eu](mailto:giulia.solda@hunimed.eu).

#### Conflict of interest

The authors declare no conflict of interest.

## Keywords

Perrault syndrome; whole-exome sequencing; *LARS2*; mutations; mitochondrial aminoacyl-tRNA synthetases

---

## Introduction

The association of gonadal dysgenesis and deafness was firstly reported in 1951 and has later been referred to as Perrault syndrome (MIM #233400) <sup>1</sup>. It is a rare autosomal recessive disorder characterized by ovarian dysgenesis with normal karyotype (46, XX) and primary ovarian insufficiency in females, and by bilateral sensorineural hearing loss (HL) in both genders. Severity of HL may range from moderate with early-childhood onset to profound with prelingual onset. Additionally, variable neurological symptoms may be present in some families, such as intellectual disability, developmental delay, muscle weakness, cerebellar ataxia, and peripheral sensorimotor neuropathy. In general, sensorineural HL is the first clinical manifestation, although a formal diagnosis of Perrault syndrome will not be made until a failure of puberty (primary amenorrhea) or a secondary amenorrhea is noted in affected young women <sup>2</sup>.

The genetic and molecular bases of Perrault syndrome have long remained unknown; the advent of next-generation sequencing (NGS) has been fundamental to allow comprehensive genetic analysis and gene discovery for such rare inherited condition, irrespective of preexisting linkage data in a patient's family. Indeed, in the last few years, causative mutations were identified in five genes: *HSD17B4* (17-beta hydroxysteroid dehydrogenase 4; MIM \*601860), *HARS2* (mitochondrial histidyl-tRNA synthetase; MIM \*600783), *LARS2* (mitochondrial leucyl-tRNA synthetase; MIM \*604544), *CLPP* (mitochondrial ATP-dependent chambered protease; MIM \*601119), and *C10ORF2* (mitochondrial DNA helicase Twinkle; MIM\*606075) <sup>3-7</sup>. Notably, four of them are nuclear genes coding for mitochondrial proteins, pointing to an important role for these organelles in the maintenance of normal hearing and ovarian function. However, the so-far identified Perrault-syndrome genes collectively explain only a fraction of cases (ten families worldwide, of the 17 so-far genetically analyzed by NGS), suggesting that additional disease-causing genes still remain to be discovered <sup>2,6-8</sup>.

Here, we sought to determine the molecular basis of Perrault syndrome in one non-consanguineous Italian family by whole-exome sequencing (WES).

## Materials and Methods

### Clinical evaluation

One Italian Perrault syndrome family, with two affected (one male, II1; and one female, II3) and two healthy siblings, was recruited. The study was approved by the Ethical Committee of the Fondazione IRCCS Cà Granda Ospedale Maggiore Policlinico of Milan and performed according to the Declaration of Helsinki. DNA samples were obtained after having acquired a written informed consent from all participants and anonymized according to the Italian legislation on sensible data recording.

The female proband (II3) presented with premature ovarian failure at 31 years and profound congenital HL (Supplementary Figure S1). She had menarche at the age of 13 years and regular menses until the age of 28 years, when she experienced phases of polymenorrhea and oligomenorrhea before being hospitalized for secondary amenorrhea. In that occasion, she presented with high levels of follicle-stimulating and luteinizing hormones (118 IU/l and 45.4 IU/l, respectively), and concomitant decrease of estradiol levels (<20 pg/ml). Abdominal ultrasounds evidenced a bicornuate uterus, hypoplastic left ovary, and probable dysgenesis of the right ovary, which could not be visualized. The proband's oldest brother (II1) was diagnosed with congenital bilateral profound sensorineural HL (Supplementary Figure S1). Both siblings had normal speech development, and received bilateral cochlear implants. Both have normal karyotype (as assessed by cytogenetic analysis), neurological, and cognitive function. A maternal cousin, not available to the study, was referred to have congenital hypoacusia, mental retardation, and café-au-lait spots.

### Genetic analyses

WES was performed on five family members at the service facility of the Yale Center for Genome Analysis. Briefly, 75-bp paired-end libraries were constructed starting from 1 µg of blood-derived genomic DNA, and captured on biotinylated DNA baits using the SeqCap EZ Human Exome Library v.2.0 (Roche NimbleGen, Basel, Switzerland). After streptavidin-based purification, amplification, and barcoding, samples were run on a single lane of an HiSeq 2000 (Illumina, San Diego, CA, USA). Quality control, alignment to the human reference genome (hg19, GRCh37 build), and variant calling were performed in October 2013 using the Whole-Exome sequencing Pipeline web tool <sup>9</sup>.

For the prioritization of potentially pathogenic variants, artefacts were filtered out by comparison with exomes sequenced at the same service facility for other conditions. Nonsense, frameshift, and canonical splice site variants (*i.e.* variants within 2 base pairs from splice sites) were considered as more likely to be deleterious. Common single nucleotide variants (SNVs) and insertion-deletions were excluded by filtering against 1000 Genome Project, National Heart, Lung, and Blood Institute Exome Sequencing Project (NHLBI-ESP; 6500 exomes), and dbSNP135 (except variants flagged as clinically relevant) databases. The threshold for the maximum minor allele frequency (MAF) was set to 1% <sup>10</sup>. Consistently with a recessive inheritance model, only homozygous or compound heterozygous variants shared among affected individuals were considered. Potential pathogenicity of SNVs was assessed using SIFT <sup>11</sup>, MutationTaster2 <sup>12</sup>, PolyPhen-2 <sup>13</sup>, MutationAssessor <sup>14</sup>, FATHMM <sup>15</sup>, Likelihood Ratio Test (LRT) <sup>16</sup>, and Condel <sup>17</sup>.

### Sanger sequencing

*LARS2* exons 10 and 17 were PCR amplified using sets of primers designed on the basis of the known genomic sequence of the gene (GenBank accession number NG\_033907.1). PCRs were performed on 10-20 ng of genomic DNA, following standard procedures. Primer sequences, as well as the specific PCR conditions for each primer couple are available on request.

Direct sequencing of amplified fragments was performed on both strands as described <sup>18</sup>.

Pathogenic variants were submitted to the NCBI ClinVar database (accession numbers SCV000238519-21).

### In-silico protein analysis and homology modeling

*In-silico* analyses of remote homology were performed on the editing and Leucin-Specific (LS) domains, using as queries human LARS2 and *E. coli* LeuRS amino acid sequences (UniProt accession numbers Q15031 and P07813), as described <sup>6</sup>. Briefly, each sequence was aligned by the HHblits algorithm <sup>19</sup> to all possible similar sequences from bacteria, fungi, and protists, producing a *consensus* sequence that highlights, for each residue, the underlying homology among species. Homology modeling was performed by I-TASSER <sup>20</sup>, using as templates the *E. coli* LeuRS in either the aminoacylation or the editing conformation (PDB entries 4AQ7 and 4ARI, respectively) and the FoldX algorithm for structure optimization and *in-silico* mutagenesis.

## Results

### Exome sequencing identifies two novel potentially pathogenic missense variants in LARS2

WES, performed on five family members (I1, I2, II1, II2, II3, Fig. 1A), yielded on average 5.2 Gb high quality sequence data per exome, with about 98.9% coverage of the target and a 70× mean coverage (range 51×-81×), with more than 93% of target covered >10× (Supplementary Table S1). Exome analysis (Supplementary Table S2) revealed that both affected siblings were compound heterozygous for two novel missense variants in *LARS2*: a NM\_015340.3:c.899C>T transition (p.Thr300Met), which was inherited from their mother, and a NM\_015340.3:c.1912G>A transition (p.Glu638Lys), which was inherited from their father (Figure 1A). The p.Thr300Met variant was predicted to be damaging by all programs except FATHMM, whereas the p.Glu638Lys variant was predicted to be deleterious by five (SIFT, Polyphen HumVar, Polyphen HumDiv, MutationTaster, LRT) out of eight programs (Supplementary Table S3). The presence of candidate variants and cosegregation with the phenotype in all family members were confirmed by Sanger sequencing (Figure 1A). In addition, the identified missense variants are absent both in an in-house database of about 3500 ethnically-matched control exomes and in the Exome Aggregation Consortium (ExAC) browser, which includes data from more than 60,000 individuals (<http://exac.broadinstitute.org/>, last accessed August 2015), suggesting that they likely represent private mutations.

### Protein sequence analysis and molecular modeling support the pathogenicity of identified variants

The *LARS2* gene localizes on chromosome 3 and codes for a 903-amino-acid long mitochondrial leucyl-tRNA synthetase, which belongs to the class 1 of aminoacyl-tRNA synthetases. Aminoacyl-tRNA synthetases are essential enzymes that charge the tRNA with its cognate amino acid, thus providing the substrates for protein synthesis. The *LARS2* protein (LeuRS) is composed of five principal domains, known as catalytic, editing, LS, anticodon-recognition, and C-terminal (C-ter) domains (Figure 1B), and two catalytically important motifs, namely the HIGH sequence -at the amino terminus- and the KMSKS loop, responsible for the binding of the 3' end of the tRNA during aminoacylation. The enzyme,

similar to several other aminoacyl-tRNA synthetases, can exist in two different conformations: the aminoacylation and the editing ones. While in the former the KMSKS loop moves as an integral part of the LS domain and closely interacts with the 3' end of the tRNA, thus promoting catalysis, in the latter it remains in an open, relaxed conformation with no contacts to the 3' end of the acceptor stem <sup>21</sup>.

The site of one of the mutant residues, p.Glu638, is highly conserved across eukaryotes, from yeast to humans. In particular, it is located in the catalytic domain just upstream of the KMSKS loop (Figure 1B). In contrast, the other mutant residue, p.Thr300, is located within the editing domain and is conserved in mammals, but not in more distantly-related species (Supplementary Figure S2). However, due to the ancient evolutionary origin of aminoacyl-tRNA synthetases, the interpretation of missense mutations in these genes is particularly challenging, as single protein domains can maintain a conserved three dimensional structure without a strong conservation of the amino acid sequence. This may explain also why some of the commonly used programs to predict the deleteriousness of a given amino acid substitution fail to recognize candidate *LARS2* mutations as damaging (Supplementary Table S3). To circumvent this problem, we applied a sequence-alignment method that detects remote homology and builds consensus profiles of highly diverse sequences <sup>19</sup>. This analysis revealed that p.Thr300 and p.Glu638 correspond to the consensus amino acid for both the human-based and *E. coli*-based alignments, suggesting the functional and possibly structural relevance of these residues (Figure 1C). In addition, neither methionine nor lysine are seen in any species at positions p.Thr300 and p.Glu638, respectively.

To predict the consequences of the newly identified variants on the *LARS2* protein structure, molecular models of the human protein (Figure 2A) were built by homology modeling, using as templates the *E. coli* LeuRS in either the aminoacylation or the editing conformation.

Residue p.Thr300 is part of a conserved threonine-rich region that shapes the pocket of the amino acid binding in the LeuRS editing site (Figure 2B). Mutation of this threonine to a methionine could either interfere with the cleavage of the incorrectly paired aminoacyl-tRNA molecule, or perturb the discrimination of the cognate amino acid, possibly leading to leucine hydrolyzation from Leu-tRNA<sup>Leu</sup>.

Residue p.Glu638 is adjacent to the conserved and catalytically important 639-KMSKS-643 loop. This loop, which plays a critical role in the activation and aminoacylation reactions, can adopt three conformational states: open, semi-open and closed, depending on the functional configuration of the enzyme. In the aminoacylation configuration, the KMSKS loop is in a fully closed state and forms base-specific interactions with the adenine base at the 3' of the tRNA, whereas in the editing configuration it is in a fully open state, unable to form specific interactions to the adenine. The movement from the editing to the aminoacylation configuration brings the loop closer to the active site, allowing it to make critical interactions with the 3' strand, which correctly position the tRNA extremity for the transfer reaction. In particular, p.Glu638 salt bridges with p.Lys644 at the other edge of the loop, possibly helping the full closure of the loop and stabilizing the closed conformation (Figure 2C). The p.Glu638Lys mutation will disallow the interaction with residue p.Lys644,

and the charge repulsion will probably interfere with the conformational change from the open to the closed state.

## Discussion

Mutations in *LARS2* were only recently identified as responsible for Perrault syndrome in two families, one of Palestinian and one of Slovenian ancestry<sup>6</sup>, in which a total of three genetic defects were reported (Table 1). Here, we describe two novel disease-causing variants, thus providing the first independent replication of the involvement of *LARS2* in Perrault syndrome pathogenesis, and significantly expanding the current spectrum of pathogenic mutations for this gene (Table 1). Interestingly, the newly reported mutations occur in the editing and near the Leucine-Specific domain, consistent with two of the three previously-reported mutations (Figure 1B). In particular, p.Thr300Met affects the pocket of the amino acid binding in the LeuRS editing site: we thus hypothesize that this residue could be important for the proofreading mechanism of the enzyme. On the basis of experiments monitoring the deacylation of Ile-tRNA<sup>Leu</sup>, it has been proposed that the editing site of human LeuRS is not operational<sup>22</sup>. However, more recent in-depth kinetic analyses established that the physiological target for *E. coli* LeuRS translational quality control is norvaline, a side product of the leucine biosynthetic pathway that accumulates under limited-oxygen growth conditions, suggesting that the LeuRS editing has been evolutionary optimized to eliminate non-proteinogenic norvaline rather than isoleucine<sup>23</sup>. Hence, the prime biological importance of the editing domain of LeuRS might consist in excluding from protein synthesis a range of non-proteinogenic amino acids (including norvaline), which are ubiquitous in many cellular metabolic pathways and can accumulate in stress conditions or can be taken up in the diet<sup>24</sup>.

Mutations in almost every nuclear-encoded mitochondrial aminoacyl-tRNA synthetase (18 out of 19) are associated with a wide variety of syndromes and diseases, all caused by defective aminoacylation activity of the corresponding enzyme<sup>25,26</sup>. Usually, defects in each synthetase result either in a tissue-specific disease, most commonly affecting the central nervous system, or in a syndromic condition. Apart from *HARS2* and *LARS2*, only mutations in an additional mitochondrial tRNA synthetase (*AARS2*) seem to affect gonadal function<sup>27</sup>, whereas deafness is reported in patients with mutations in *SARS2*, *FARS2*, *IARS2*, *NARS2*, and the dual-localized (mitochondrial and cytoplasmic) *KARS*<sup>25,28-30</sup>. However, at present, the number of patients with mutations in different mitochondrial aminoacyl-tRNA synthetases is too small to provide conclusive evidence of robust genotype-phenotype correlations.

Concerning genotype-phenotype correlations in *LARS2*-dependent Perrault syndrome, the here-described Italian proband shows a more severe audiological phenotype (congenital profound HL affecting all frequencies), but a milder ovarian phenotype (normal menarche at age 13 and primary ovarian insufficiency at 28 y.o.) compared with previously-reported cases (Table 1). Moreover, to our knowledge, the presence of bicornuate uterus has never been associated with the Perrault syndrome phenotype before. These observations suggest the existence of a certain degree of clinical variability, which may be related to the specific

genetic alteration and/or cell type-specific mitochondrial functions, metabolite requirements, as well as differential expression in basal mRNA levels of tRNA synthetases.

## Supplementary Material

Refer to Web version on PubMed Central for supplementary material.

## Acknowledgements

This study was supported by the Italian Telethon Foundation grant GGP11177 and Fondazione Cariplo grant N°2013-0825. We are indebted to all the subjects who participated in the study. We thank Manuela Seia, Cristina Curcio, and Elena Benzoni for collaboration in the collection of DNA samples.

## References

- Perrault M, Klotz B, Housset E. Deux cas de syndrome de Turner avec surdi-mutité dans une meme fratrie. *Bull. Mem. Soc. Med. Hop. Paris.* 1951; 16:79–84. [PubMed: 14821788]
- Newman, WG.; Friedman, TB.; Conway, GS. Perrault Syndrome. In: Pagon, RA.; Adam, MP.; Ardinger, HH.; Wallace, SE.; Amemiya, A.; Bean, LJH., et al., editors. *GeneReviews® Internet.* University of Washington, Seattle; Seattle (WA): 1993-2015. 2014 Sep 25 Available from <http://www.ncbi.nlm.nih.gov/books/NBK242617/>
- Pierce SB, Walsh T, Chisholm KM, Lee MK, Thornton AM, Fiumara A, et al. Mutations in the DBP-deficiency protein HSD17B4 cause ovarian dysgenesis, hearing loss, and ataxia of Perrault Syndrome. *Am. J. Hum. Genet.* 2010; 87:282–288. [PubMed: 20673864]
- Pierce SB, Chisholm KM, Lynch ED, Lee MK, Walsh T, Opitz JM, et al. Mutations in mitochondrial histidyltRNA synthetase HARS2 cause ovarian dysgenesis and sensorineural hearing loss of Perrault syndrome. *Proc. Natl. Acad. Sci. U. S. A.* 2011; 108:6543–6548. [PubMed: 21464306]
- Jenkinson EM, Rehman AU, Walsh T, Clayton-Smith J, Lee K, Morell RJ, et al. Perrault syndrome is caused by recessive mutations in CLPP, encoding a mitochondrial ATP-dependent chambered protease. *Am. J. Hum. Genet.* 2013; 92:605–613. [PubMed: 23541340]
- Pierce SB, Gersak K, Michaelson-Cohen R, Walsh T, Lee MK, Malach D, et al. Mutations in LARS2, encoding mitochondrial leucyl-tRNA synthetase, lead to premature ovarian failure and hearing loss in Perrault syndrome. *Am. J. Hum. Genet.* 2013; 92:614–620. [PubMed: 23541342]
- Morino H, Pierce SB, Matsuda Y, Walsh T, Ohsawa R, Newby M, et al. Mutations in Twinkle primase-helicase cause Perrault syndrome with neurologic features. *Neurology.* 2014; 83:2054–2061. [PubMed: 25355836]
- Ahmed S, Jelani M, Alrayes N, Mohamoud HS, Almramhi MM, Anshasi W, et al. Exome analysis identified a novel missense mutation in the CLPP gene in a consanguineous Saudi family expanding the clinical spectrum of Perrault Syndrome type-3. *J. Neurol. Sci.* 2015; 353:149–154. [PubMed: 25956234]
- D’Antonio M, D’Onorio De Meo P, Paoletti D, Elmi B, Pallocca M, Sanna N, et al. WEP: a high-performance analysis pipeline for whole-exome data. *BMC Bioinformatics.* 2013; 14(Suppl 7):S11. [PubMed: 23815231]
- Bamshad MJ, Ng SB, Bigham AW, Tabor HK, Emond MJ, Nickerson DA, et al. Exome sequencing as a tool for Mendelian disease gene discovery. *Nat. Rev. Genet.* 2011; 12:745–755. [PubMed: 21946919]
- Sim NL, Kumar P, Hu J, Henikoff S, Schneider G, Ng PC. SIFT web server: predicting effects of amino acid substitutions on proteins. *Nucleic. Acids. Res.* 2012; 40:W452–W457. [PubMed: 22689647]
- Schwarz JM, Cooper DN, Schuelke M, Seelow D. MutationTaster2: mutation prediction for the deep-sequencing age. *Nat. Methods.* 2014; 11:361–362. [PubMed: 24681721]
- Adzhubei I, Jordan DM, Sunyaev SR. Predicting functional effect of human missense mutations using PolyPhen-2. *Curr. Protoc. Hum. Genet.* 2013; 76:7.20.1–7.20.41. [PubMed: 23315928]

14. Reva B, Antipin Y, Sander C. Predicting the functional impact of protein mutations: application to cancer genomics. *Nucleic. Acids. Res.* 2011; 39:e118. [PubMed: 21727090]
15. Shihab HA, Gough J, Cooper DN, Stenson PD, Barker GLA, Edwards KJ, et al. Predicting the Functional, Molecular and Phenotypic Consequences of Amino Acid Substitutions using Hidden Markov Models. *Hum. Mutat.* 2013; 34:57–65. [PubMed: 2303316]
16. Chun S, Fay JC. Identification of deleterious mutations within three human genomes. *Genome. Res.* 2009; 19:1553–1561. [PubMed: 19602639]
17. González-Pérez A, López-Bigas N. Improving the Assessment of the Outcome of Nonsynonymous SNVs with a Consensus Deleteriousness Score, *Condel.* *Am. J. Hum. Genet.* 2011; 88:440–449. [PubMed: 21457909]
18. Robusto M, Fang M, Asselta R, Castorina P, Previtali SC, Caccia S, et al. The expanding spectrum of PRPS1-associated phenotypes: three novel mutations segregating with X-linked hearing loss and mild peripheral neuropathy. *Eur. J. Hum. Genet.* 2015; 23:766–773. [PubMed: 25182139]
19. Remmert M, Biegert A, Hauser A, Söding J. HHblits: lightning-fast iterative protein sequence searching by HMM-HMM alignment. *Nat. Methods.* 2011; 9:173–175. [PubMed: 22198341]
20. Yang J, Yan R, Roy A, Xu D, Poisson J, Zhang Y. The I-TASSER Suite: Protein structure and function prediction. *Nat. Methods.* 2015; 12:7–8. [PubMed: 25549265]
21. Palencia A, Crépin T, Vu MT, Lincecum TL Jr, Martinis SA, Cusack S. Structural dynamics of the aminoacylation and proofreading functional cycle of bacterial leucyl-tRNA synthetase. *Nat. Struct. Mol. Biol.* 2012; 19:677–684. [PubMed: 22683997]
22. Lue SW, Kelley SO. An aminoacyl-tRNA synthetase with a defunct editing site. *Biochemistry.* 2005; 44:3010–3016. [PubMed: 15723544]
23. Cvetesic N, Palencia A, Halasz I, Cusack S, Gruic-Sovulj I. The physiological target for LeuRS translational quality control is norvaline. *EMBO. J.* 2014; 33:1639–1653. [PubMed: 24935946]
24. Dunlop RA, Cox PA, Banack SA, Rodgers KJ. The non-protein amino acid BMAA is misincorporated into human proteins in place of L-serine causing protein misfolding and aggregation. *PLoS. ONE.* 2013; 8:e75376. [PubMed: 24086518]
25. Yao P, Fox PL. Aminoacyl-tRNA synthetases in medicine and disease. *EMBO. Mol. Med.* 2013; 5:332–343. [PubMed: 23427196]
26. Euro L, Konovalova S, Asin-Cayuela J, Tulinius M, Griffin H, Horvath R, et al. Structural modeling of tissue-specific mitochondrial alanyl-tRNA synthetase (AARS2) defects predicts differential effects on aminoacylation. *Front. Genet.* 2015; 6:21. [PubMed: 25705216]
27. Dallabona C, Diodato D, Kevelam SH, Haack TB, Wong LJ, Salomons GS, et al. Novel (ovario) leukodystrophy related to AARS2 mutations. *Neurology.* 2014; 82:2063–2071. [PubMed: 24808023]
28. Schwartzenruber J, Buhas D, Majewski J, Sasarman F, Papillon-Cavanagh S, Thiffault I, et al. Mutation in the nuclear-encoded mitochondrial isoleucyl-tRNA synthetase IARS2 in patients with cataracts, growth hormone deficiency with short stature, partial sensorineural deafness, and peripheral neuropathy or with Leigh syndrome. *Hum Mutat.* 2014; 35:1285–1289. [PubMed: 25130867]
29. Simon M, Richard EM, Wang X, Shahzad M, Huang VH, Qaiser TA, et al. Mutations of human NARS2, encoding the mitochondrial asparaginyl-tRNA synthetase, cause nonsyndromic deafness and Leigh syndrome. *PLoS Genet.* 2015; 11:e1005097. [PubMed: 25807530]
30. Santos-Cortez RL, Lee K, Azeem Z, Antonellis PJ, Pollock LM, Khan S, et al. Mutations in KARS, encoding lysyl-tRNA synthetase, cause autosomal-recessive nonsyndromic hearing impairment DFNB89. *Am J Hum Genet.* 2013; 93:132–140. [PubMed: 23768514]



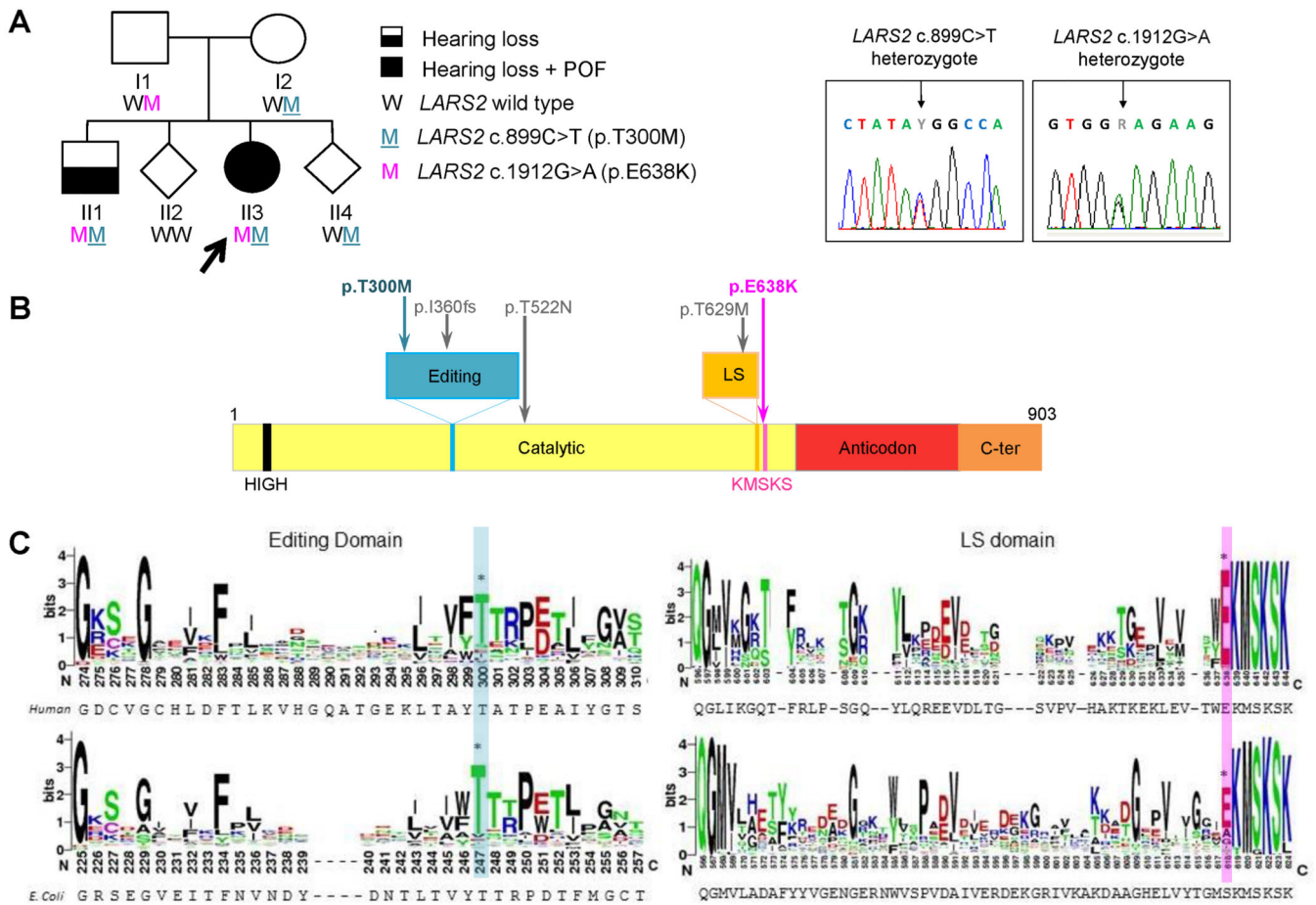


**Figure 1. Family segregation and *in-silico* analyses of the newly-identified mutations responsible for Perrault syndrome**

**A.** *LARS2* mutations segregating with Perrault syndrome in the analyzed family. (left) Pedigree of the family under study. The gender of proband's unaffected siblings is not reported to anonymize the family tree. Genotypes are indicated below each symbol (W, wild-type alleles, M, mutant alleles). The arrow indicates the proband (II3). Half-filled and filled symbols denote the sole presence of hearing loss and the concomitant presence of hearing loss and premature ovarian failure, respectively. On the right, electropherograms of the regions surrounding the identified mutations in the *LARS2* gene are shown. The positions of the C>T and G>A transitions (numbered according to NM\_015340.3 cDNA) is indicated by an arrow. Y = C or T; R = G or A. **B.** Schematic representation of the *LARS2* protein showing the position of the newly-identified mutations as well as the previously-reported ones. The editing and the Leucine-Specific (LS) domains of the protein are enlarged to better visualize the location of mutant residues. The positions of the HIGH and KMSKS motifs are also reported. **C.** Consensus sequences of *LARS2* Leucine-Specific and Editing (partial) domains from alignments to humans (upper) and *E. coli* (lower). Sequence analysis was based on remote homology of the amino acid regions surrounding the identified mutations by using the HHblits algorithm. Consensus sequences are displayed with WebLogo. The position of the residues involved in the mutations are shaded.

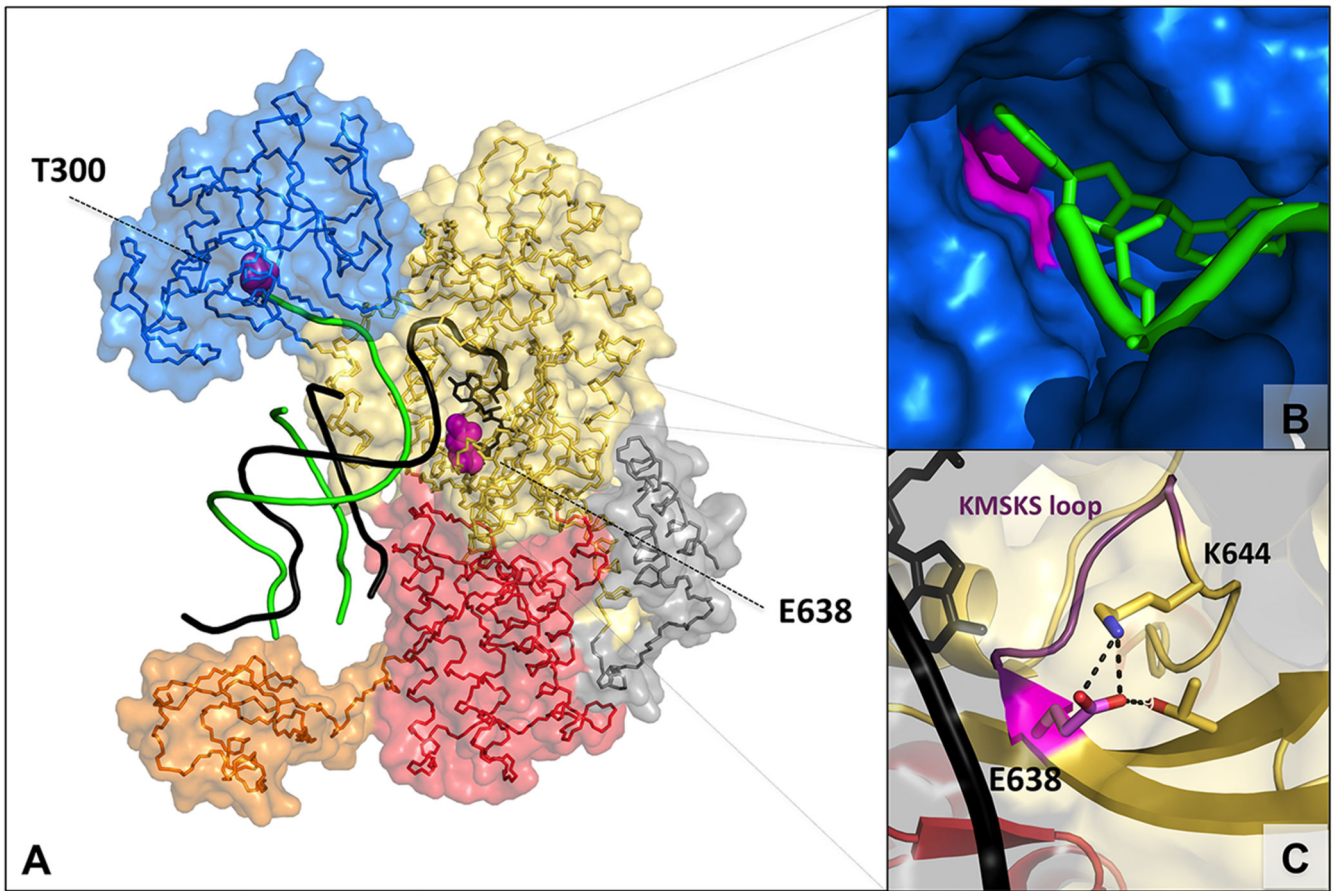


**Figure 2. Structural analysis of LARS2 amino acids affected by novel Perrault syndrome mutations**

**A.** Surface representation of human mitochondrial LeuRS in the aminoacylation conformation (model based on *E. coli* 4AQ7 pdb structure), showing the different domains coloured as follows: grey, N-terminal; yellow, catalytic; cyan, editing; red, anticodon-binding; orange, C-terminal. The tRNA<sup>Leu</sup> (black ribbon), and the leucine-adenylate analogue (black sticks) are docked in the catalytic domain. The mutated residues are highlighted in magenta, with their atoms drawn as Van der Waals spheres. For clarity purposes, the tRNA<sup>Leu</sup> in the editing conformation is also included and shown as green ribbon (from 4ARI pdb structure). **B.** Surface representation of the amino acid binding pocket of the editing site in the editing conformation (human model based on *E. coli* LeuRS 4ARI pdb structure), with tRNA<sup>Leu</sup> docked into it (green stick). Residue p.Thr300 (magenta) is part of the pocket, coordinating the binding of the substrate. **C.** Ribbon representation of part of the catalytic domain surrounding residue p.Glu638, in the aminoacylation conformation (human model based on *E. coli* 4AQ7 pdb structure). The residues of the KMSKS motif are coloured pink. Residue p.Glu638 is salt bridging p.Lys644 at the edge of the KMSKS loop, stabilizing its closed state. H-bond between p.Glu638 and p.Thr603 is also highlighted.

**Table 1**  
**Molecular and clinical features of *LARS2*-dependent Perrault syndrome probands**

1A. Summary of demographic and molecular features							
Patient	Sex	Family ancestry	Consanguinity	hg19 coordinates	Mutation cDNA <sup>1</sup> (protein)	Karyo-type	Ref.
<i>P1</i>	F	Palestinian	Y	chr3: 45537808	c.1565C>A <sup>2</sup> (p.Thr522Asn)	46, XX	[6]
<i>P2</i>	F	Slovenian	N	chr3: 45527242 chr3: 45557610	c.1077delT (p.Ile360PhefsTer15) c.1886C>T (p.Thr629Met)	46, XX	
<i>P3</i>	F	Italian	N	chr3: 45518000 chr3: 45557636	c.899C>T (p.Thr300Met) c.1912G>A (p.Glu638Lys)	46, XX	This study

1B. Summary of clinical features						
Patient	HL onset	Audiological features	FSH/LH hormone levels (age)	Ovarian phenotype	Uterine phenotype	Neurological symptoms
<i>P1</i>	3-5 y.o.	Right ear: severe HL with upsloping audiogram; Left ear: mild HL	FSH: 76.9 IU/l LH: 30.3 IU/l (17 y.o.)	Primary amenorrhea at 17 y.o. Ovarian dysgenesis	Small prepubertal uterus	N
<i>P2</i>	n.r.	Bilateral severe sensorineural HL	FSH: 101 IU/l LH: n.r. (30 y.o.)	Menarche at 13 y.o. Primary ovarian insufficiency at 19 y.o.	None	N
<i>P3</i>	congenital	Bilateral progressive profound sensorineural HL	FSH: 118 IU/l LH: 45.4 IU/l (28 y.o.)	Menarche at 13 y.o. Primary ovarian insufficiency at 28 y.o. Hypoplasia left ovary /dysgenesis right ovary	Bicornuate uterus	N

HL: Hearing Loss; FSH: follicle-stimulating hormone; LH: luteinizing hormone; y.o.: years old; n.r.: not reported

<sup>1</sup>Numbering according to the reference sequence NM\_015340.3

<sup>2</sup>The mutation is present in the homozygous state